Asian Journal of Chemistry; Vol. 34, No. 4 (2022), 849-856

ASIAN JOURNAL OF CHEMISTRY

https://doi.org/10.14233/ajchem.2022.23571

Theoretical Insights into the Intermolecular Hydrogen Bond Effect on ESIHT Process in 2′-Hydroxychalcone: A Combined DFT/TDDFT Study

Y.L. RAMU[1,*], K. JAGADEESHA[1] and M. RAMEGOWDA[2]

[1]P.G. Department of Physics, Government College (Autonomous), Mandya-571401, India
[2]Department of Physics, Mandya University, Mandya-571401, India

*Corresponding author: E-mail: ramuylphy652@gmail.com

Received: 6 October 2021; *Accepted*: 13 December 2021; *Published online*: 10 March 2022; AJC-20725

Present computational study lighting up the ground and excited states properties of 2′-hydroxychalcone (2′-HC) and 2′-HC + $(H_2O)_2$-[2′-HCH] molecules by employing density functional theory (DFT) and time-dependent density functional theory (TD-DFT). Furthermore, micro-solvation, hydrogen bond dynamics and natural charge analysis studies have been done for both molecules at ground/excited states by using effective fragment potential (EFP1)/natural bond orbital (NBO) methods at 6-31G(d,p)/B3LYP level. The excited state intra-molecular hydrogen atom transfer (ESIHT) mechanism of 2′-HC was investigated *via* potential energy scans (PES). No hydrogen atom transfer is observed in the S_3 state of 2′-HC and S_1/S_3 states of 2′-HCH. The optimized molecular structures, molecular orbital's and electrostatic potential maps were depicted along with UV-Vis absorption spectra. Good consistency between experimental and computational absorption wavelength for a 2′-HC molecule with methanol as solvent.

Keywords: 2′-Hydroxychalcone, TD-DFT, PCM, EFP1, Effective fragment potential.

INTRODUCTION

The intra- and inter-molecular non-covalent hydrogen bond (HB) interactions at both ground and excited states play a crucial role in the photochemistry of organic and biological molecules [1-7] that have been extensively analyzed both experimentally [8-10] and theoretically [11-14]. Many theoretical investigations were performed to determine the nature of the hydrogen bonds, which depends on the electronegativity of the atoms. The excited-state hydrogen bond length can be observed when bond length increases/decreases (strengthening/weakening of HB) can lower/heighten the energy; wavelength shifted to upward/downward values followed of an increase/decrease on the absorption intensity and induced an electronic spectral red shift/blue shift [15-17]. The free radicals of donor-acceptor electrons can form hydrogen bonds, which influence their structure and fluorescent properties in their ground and higher states [18,19]. The theoretical studies of electronic structure and related phenomena using DFT/TDDFT/EFP1/PCM methods were applied to determine the interaction of chromophores with water molecules at the ground and excited states [20-22]. The EFP1 method was developed specifically for water that can be inserted with a polarizable continuum model (PCM) has been applied to study intramolecular hydrogen bonding and quantum-mechanical molecular behaviour in water [23-26].

Chalcones and its derivatives represent an important class of organic compounds that exhibit excellent pharmacological and biological activities, including anti-inflammatory [27], antimicrobial [28], antiviral [29] and antibacterial [30] activity. 2′-Hydroxychalcone (2′-HC) is a member of phenols and chalcones having an open-chain structure that contains two aromatic rings A and B bonded by three carbon atoms C7-C8=C9. 2′-Hydroxychalcone having 29 atoms in which hydroxyl group is attached to C5-position of ring-A and an intramolecular hydrogen bonding exist between the hydrogen of the hydroxyl and oxygen of the carbonyl group of basic chalcone moiety. The evaluation of toxicological effects of 2′-HC on the lipid-loaded HepG2 cells, cellular respiration, ROS production, oxidative stress, inflammation and apoptosis was studied [31]. In the gas phase and solvents, 2′-HC exhibits anti-inflammatory agent and free radical scavenging activities.

The results have shown that hydrogen atom transfer (HAT) would be the most supportive mechanism for elucidating the radical-scavenging activity [32]. 2′-Hydroxychalcone shows a significant inhibitory effect on the growth of A549 lung cancer cells [33] and also it is an ESIPT active compound with high potential application in optoelectronics and organic lasers [34]. 2′-Hydroxychalcone can readily isomerize into flavanones *i.e.* the bioactive components in food plants can assimilate dynamic processes that encompass many chemical species [35].

COMPUTATIONAL METHODS

Avogadro is a free cross-platform molecular editor and visualization used to design the pure molecule and its water complex [36]. The geometric parameters of 2′-HC and 2′-HC+ $(H_2O)_2$-[2′-HCH] were optimized with no restrictions and thrust upon the molecular structure at the time of the optimization process using MMFF94s force field. The gas-phase geometry optimization of 2′-HC and 2′-HCH molecule at the DFT [37-39] level for the ground state (S_0) and at the TDDFT [40-42] level for both first excited state (S_1) and third excited states (S_3) by using hybrid functional B3LYP with 6-31G (d,p) basis set [43-46] implemented in GAMESS-US software suite. The natural charges of 2′-HC and 2′-HCH molecules at S_0, S_1 and S_3 states were reckoned using the natural bond orbital's (NBO.6) program [47] under GAMESS software package [48,49]. The MEP and frontier molecular orbital's are plotted by wxMacMolplt. The hydrogen atom (H28) transfer mechanism in the S_1 state of pure molecule can be explained through the PES scan study. The UV-Vis spectral study was done through gas phase and polar solvents like water and ethanol with PCM/B3LYP/TDDFT/6-31G (d,p) method [50].

RESULTS AND DISCUSSION

Electronic structural studies at S_0, S_1 and S_3 states: Optimized molecular structures of 2′-HC and 2′-HCH molecules at S_0, S_1 and S_3 states were calculated using DFT/TDDFT/B3LYP/6-31G(d,p) methods and depicted in Figs. 1 and 2. At the ground state of 2′-HC and 2′-HCH molecule, an intramolecular HB exists between hydrogen (H28) of the hydroxyl group (C5-position) and oxygen (O17) of the carbonyl group (C7-position). In a micro-solvated molecule, two intermolecular HB's arise across the hydroxyl group and carbonyl group, along with one hydrogen bond between water molecules. When 2′-HC experience photoinduction, structural parameters of the 2′-HC molecule changes both in bond lengths and bond angles. In aromatic ring-A, C1=C2, C3=C4, C5=C6 bond lengths increased and C2=C3 bond length decreased in S_1, S_3 states. Whereas C4-C5 bond length increased in S_1 state but decreased in S_3 state and C1-C6, C5=O16 bond lengths decreased in S_1 state but increased in S_3 state. In aromatic ring-B, C11=C12, C14-C15 bond lengths decreased and C10-C11, C12-C13, C13=C14, C15=C10 bond lengths increased in S_1, S_3 states. In the alkyl chain, the bond lengths of C7=C8, C9-C10 decreased and C8-C9/C7-O17 bond lengths increased in S_1, S_3 states. The C-H bond lengths vary in the range 0-3 × 10^{-3} Å in both excited states. The bond angles between the respective atoms vary in the range 0-5.6º/0-2.6º in S_1/S_3 states. Under the influence of micro-solvation, 2′-HCH molecular structural parameters reform. In aromatic ring-A, C1-C2, C3-C4, C5-O16, O16-H28/C4=C5, C5-C6, C1=C6 bond lengths decreases/increases. Whereas in aromatic ring-B, C10=C11 and C13-C14 bond lengths decreases and the other covalent bond lengths remain unchanged. In alkyl chain, C6-C7, C8=C9, C7=O17/C7-C8, C9-C10 bond lengths decreases/increases. Here, C-H bond lengths vary in the range (0-0.3) Å and bond angles vary in the range 0-2.8º.

When 2′-HCH experiences photo-induction, structural parameters of 2′-HCH molecule change in bond lengths and bond angles in both the excited states. No alteration in covalent bonds was observed in both S_1 and S_3 states. In aromatic ring-A, C3-C4, C1=C6, O16-H28, C4=C5 and C2=C3, bond lengths increased in the S_1 state but decreased in the S_3 state. Whereas C1-C2, C5-C6, C5-O16 bond lengths decreased in the S_1 state

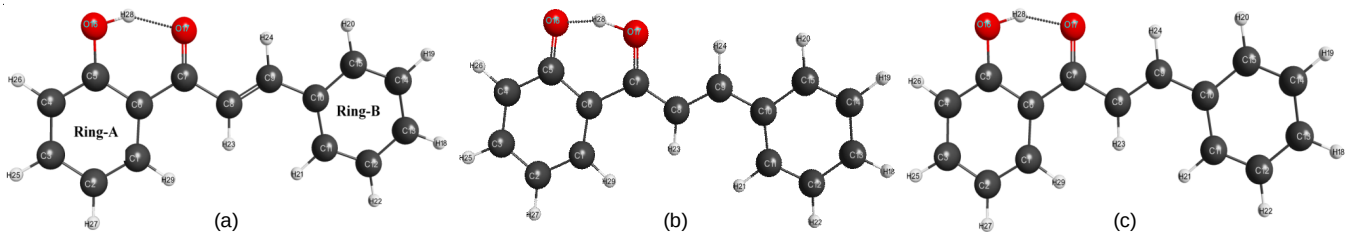

Fig. 1. Optimized molecular structures of 2'-HC molecule at (a) S_0 (b) S_1 (c) S_3 states

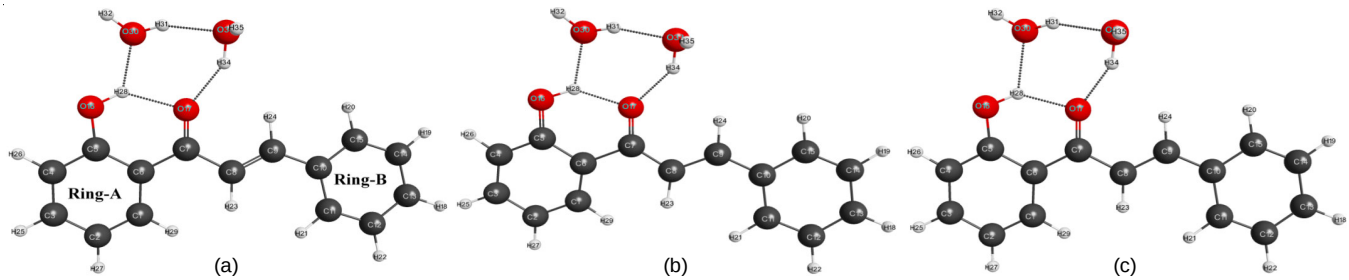

Fig. 2. Optimized molecular structures of 2'-HCH molecule at (a) S_0 (b) S_1 (c) S_3 states

but increased in the S_3 state. In aromatic ring-B, C12=C13 bond length increased in S_1, S_3 states. C11-C12, C14=C15 bond lengths increased/decreased and C10=C11, C13-C14, C10-C15 bond lengths decreased/increased in S_1/S_3 states. In alkyl chain, the bond lengths of C6-C7, C7-C8, C9-C10 decrease and C8=C9, C7=O17 increase in both excited states. The C-H bond lengths vary in the range (0-4) × 10^{-3} Å and (1-3) × 10^{-3} Å in both excited states. The bond angles vary in the range 0-8.6º/ 0-2.1º in S_1/S_3 states. The structural parameters of 2′-HC, 2′-HCH molecules at S_0, S_1 and S_3 states are presented in Tables 1 and 2.

TABLE-1
SELECTED BOND LENGTHS - r (Å) OF 2′-HC AND 2′-HCH MOLECULES AT S_0, S_1 AND S_3 STATES

r (Å)	2′-HC			2′-HCH		
	S_0	S_1	S_3	S_0	S_1	S_3
R(1-2)	1.384	1.443	1.390	1.383	1.445	1.388
R(2-3)	1.405	1.376	1.399	1.405	1.381	1.398
R(3-4)	1.385	1.409	1.400	1.383	1.395	1.400
R(4-5)	1.407	1.431	1.403	1.411	1.434	1.407
R(5-6)	1.429	1.435	1.434	1.430	1.430	1.432
R(1-6)	1.413	1.372	1.426	1.415	1.366	1.430
R(6-7)	1.475	1.514	1.456	1.473	1.549	1.469
R(7-8)	1.477	1.401	1.464	1.483	1.405	1.454
R(8-9)	1349	1.398	1.392	1.348	1.404	1.396
R(9-10)	1.461	1.426	1.429	1.462	1.422	1.427
R(10-11)	1.410	1.424	1.440	1.409	1.427	1.439
R(11-12)	1.390	1.387	1.382	1.390	1.387	1.383
R(12-13)	1.399	1.402	1.404	1.399	1.402	1.404
R(13-14)	1.396	1.402	1.412	1.395	1.403	1.411
R(14-15)	1.393	1.386	1.381	1.393	1.385	1.380
R(10-15)	1.408	1.423	1.431	1.408	1.426	1.432
R(7-17)	1.253	1.300	1.281	1.246	1.265	1.272
R(5-16)	1.336	1.292	1.337	1.330	1.310	1.332
R(16-28)	0.999	1.327	1.012	0.982	1.011	0.989
R(1-29)	1.084	1.086	1.085	1.084	1.083	1.084
R(2-27)	1.085	1.084	1.086	1.085	1.085	1.085
R(3-25)	1.087	1.086	1.086	1.087	1.084	1.086
R(4-26)	1.085	1.085	1.085	1.085	1.085	1.085
R(8-23)	1.383	1.083	1.084	1.083	1.083	1.083
R(9-24)	1.089	1.087	1.087	1.089	1.087	1.086
R(11-21)	1.086	1.086	1.085	1.086	1.086	1.085
R(12-22)	1.086	1.087	1.086	1.086	1.087	1.086
R(13-18)	1.086	1.086	1.086	1.086	1.086	1.086
R(14-19)	1.086	1.087	1.086	1.086	1.087	1.086
R(15-20)	1.087	1.087	1.086	1.087	1.088	1.086

Natural charge analysis: NBO.6 computations have been effectuating to examine the natural charge on various atoms, rings and functional groups of 2′-HC and 2′-HCH molecules by DFT/TDDFT/B3LYP/6-31G (d,p) method at S_0, S_1 and S_3 states and are assorted in Table-3. When 2′-HC molecule undergo photo-excitation, the net natural charge on ring-A/ring-B increased by -0.302e/-0.061e in S_1 state but decreased by -0.040e/ -0.126e in S_3 state. The net natural charge of the alkyl chain increased by -0.374e, 0.141e in S_1, S_3 states. Herein, the S_1 state, hydrogen atom transfer from hydroxyl group to carbonyl group due to the effect of charge on O16 decreased by -0.034e and that on O17/H28 increased by -0.029e/0.013e. Whereas in S_3 state, the charge on O16/O17 increased by -0.009e/ -0.043e

TABLE-2
SELECTED BOND ANGLES – A (°) OF 2′-HC AND 2′-HCH MOLECULES AT S_0, S_1 AND S_3 STATES

A (°)	2′-HC			2′-HCH		
	S_0	S_1	S_3	S_0	S_1	S_3
A(1-2-3)	119.4	119	119.7	119.1	120.0	119.2
A(2-3-4)	120.7	119.7	120.0	120.6	118.3	120.0
A(3-4-5)	120.3	121.9	121.0	121.1	121.5	121.7
A(4-5-6)	119.8	117.8	120.0	119.0	120.3	119.2
A(5-6-1)	118.0	119.2	117.1	118.0	116.6	117.3
A(6-1-2)	121.7	122.4	122.1	122.2	123.2	122.7
A(4-5-16)	117.9	120.7	118.6	115.9	115.1	116.7
A(6-5-16)	122.3	121.6	121.4	125.1	124.5	124.1
A(5-6-7)	118.6	117.8	118.2	119.8	120.1	119.4
A(6-7-8)	120.8	124.5	121.1	120.4	121.1	120.4
A(6-7-17)	120.0	114.4	121.5	120.1	113.4	120.3
A(17-7-8)	119.2	121.1	117.4	119.5	125.5	119.3
A(7-8-9)	120.0	121.3	120.7	120.4	121.2	121.2
A(8-9-10)	128.1	127.9	125.5	128.1	128.5	126.0
A(9-10-11)	123.5	123.9	123.2	123.4	124.2	123.5
A(9-10-15)	118.3	118.9	119.6	118.4	119.1	119.4
A(10-11-12)	120.7	120.9	121.0	120.7	121.1	120.9
A(11-12-13)	120.3	120.7	120.5	120.3	121.0	120.6
A(12-13-14)	119.7	119.4	119.7	119.7	119.0	119.7
A(13-14-15)	119.9	120.3	120.4	120.0	120.5	120.4
A(14-15-10)	121.1	121.5	121.2	121.1	121.7	121.3
A(11-10-15)	118.2	117.2	117.2	118.2	116.7	117.2

TABLE-3
NATURAL CHARGES ON DIFFERENT ATOMS OF 2′-HC AND 2′-HCH MOLECULES AT S_0, S_1 AND S_3 STATES

Atomic number	2′-HC			2′-HCH		
	S_0	S_1	S_3	S_0	S_1	S_3
C1	-0.187	-0.095	-0.184	-0.182	-0.138	-0.171
C2	-0.279	-0.225	-0.249	-0.281	-0.144	-0.289
C3	-0.196	-0.246	-0.219	-0.199	-0.277	-0.201
C4	-0.296	-0.177	-0.265	-0.295	-0.160	-0.252
C5	0.399	0.386	0.369	0.403	0.403	0.362
C6	-0.224	-0.236	-0.185	-0.226	-0.165	-0.155
C7	0.521	0.497	0.374	0.524	0.475	0.380
C8	-0.308	-0.397	-0.154	-0.305	-0.440	-0.192
C9	-0.134	-0.136	-0.240	-0.145	-0.178	-0.233
C10	-0.090	-0.108	-0.003	-0.089	-0.104	-0.015
C11	-0.202	-0.215	-0.198	-0.203	-0.233	-0.204
C12	-0.236	-0.240	-0.243	-0.236	-0.241	-0.242
C13	-0.221	-0.238	-0.184	-0.223	-0.263	-0.193
C14	-0.238	-0.246	-0.228	-0.237	-0.248	-0.232
C15	-0.199	-0.201	-0.206	-0.202	-0.218	-0.207
O16	-0.691	-0.658	-0.700	-0.694	-0.607	-0.695
O17	-0.624	-0.653	-0.667	-0.658	-0.705	-0.713
H18	0.245	0.240	0.248	0.245	0.234	0.247
H19	0.247	0.242	0.252	0.247	0.236	0.251
H20	0.245	0.238	0.252	0.245	0.232	0.251
H21	0.238	0.231	0.242	0.238	0.224	0.240
H22	0.246	0.240	0.252	0.246	0.234	0.250
H23	0.226	0.226	0.216	0.227	0.213	0.216
H24	0.256	0.247	0.264	0.243	0.222	0.250
H25	0.245	0.254	0.242	0.244	0.262	0.243
H26	0.255	0.256	0.251	0.253	0.264	0.252
H27	0.244	0.250	0.241	0.243	0.255	0.243
H28	0.524	0.518	0.522	0.593	0.606	0.581
H29	0.235	0.248	0.226	0.233	0.262	0.229

and that on H28 decreased by 0.009e. So, no hydrogen atom transfer takes place in this state.

The net natural charge of ring-A decreased by -0.07e and that of ring-B/alkyl chain increased by -0.003e/-0.039e due to the effect of micro-solvation. When 2′-HCH molecule undergoes photo-excitation, the net natural charge on the ring-A decreased by -0.399e, -0.06e in S_1, S_3 states. And the net natural charge on the ring-B increased/decreased by -0.117e/-0.097e in S_1/S_3 states. Here, the charge on O17 increased in both the excited states by -0.048e and -0.055e. Charge on O16 decreased/increased by -0.087e/-0.001e and that on H28 increased/decreased by 0.013e/0.012e in S_1/S_3 states. It is observed that no hydrogen atom transfer in S_1 and S_3 states due to the effect of microsolvation.

Molecular orbitals: The electron donation and reception to the other species most easily occurs at the HOMO and LUMO and these orbital's has smaller and larger ionization energy. The four important MOs, namely, lowest [LUMO], second-lowest [LUMO+1], highest occupied MO's [HOMO] and second highest [HOMO-1] have been worked out for 2′-HC and 2′-HCH molecules. The calculated energies of these four MO's followed for 2′-HC are -2.2313, -0.6802, -5.9048 and -6.4218 eV, respectively and the energy gap between [HOMO-LUMO], [HOMO-1 – LUMO+1] for 2′-HC is 3.6737 eV, 5.7416 eV. Similarly, four MO's [LUMO], [LUMO+1], [HOMO], [HOMO-1] are worked out for 2′-HCH complex and the corresponding energies in the order are -2.1496, -0.6258, -5.7416 and -6.3946 eV. The energy gap between [HOMO-LUMO], [HOMO-1 – LUMO+1] are 3.592 eV, 5.7688 eV, respectively. It is observed that the "HOMO-LUMO" energy gap decreases by 0.0817 eV and the "HOMO-1-LUMO+1" energy gap increases by 0.0272 eV due to the effect of microsolvation. The frontier molecular orbital's for 2′-HC and 2′-HCH molecules are shown in Figs. 3 and 4.

MEP is computed at the DFT/TDDFT/B3LYP/6-31G(d,p) level by charge allocation resulting from the superposition of nuclear and electronic charges within the 2′-HC and 2′-HCH molecules. The negative (red)/positive (blue) zones of MEP were associated with nucleophilic/electrophilic reactivity of both molecules are shown in Figs. 5 and 6. The region of red colour around the O16 atom displays that potential is highly negative here, while it is slightly less negative around O17 atom of ring-A in S_0, S_1 and S_3 states of 2′-HC. In the S_1 and S_3 state of 2′-HCH, the region of red colour around O17 displays that potential is highly negative here, while it is slightly less negative around the O16 atom. Whereas, in S_0 state, the region of red colour around O16 displays that potential is highly negative here, while it is slightly less negative around O17 atom.

In 2′-HC and 2′-HCH molecules, the aromatic ring-A/ring-B/alkyl chain shows negative nature. On excitation of the 2'-HC molecule, more negative nature is observed in the S_1 state and slightly less negative nature is observed in the S_3 state of ring-A and B. In alkyl chain, a highly less negative nature is observed in the S_1 state and a slightly more negative nature is observed in the S_3 state. On excitation of 2′-HCH molecule, a highly less negative nature is observed in the S_1 state and a slightly less negative nature is observed in the S_3 state of ring-A. But in ring-B, slightly more negative nature is observed in the S_1 state and slightly less negative nature is observed in the S_3 state. Whereas, in alkyl chain, a highly more negative nature is observed in both S_1 and S_3 states. This is due to the reallocation of charges in both the pure and its water complex.

UV-Vis spectral analysis: The UV-Vis spectral exploration of pure and hydrated molecules in the gas phase, water and

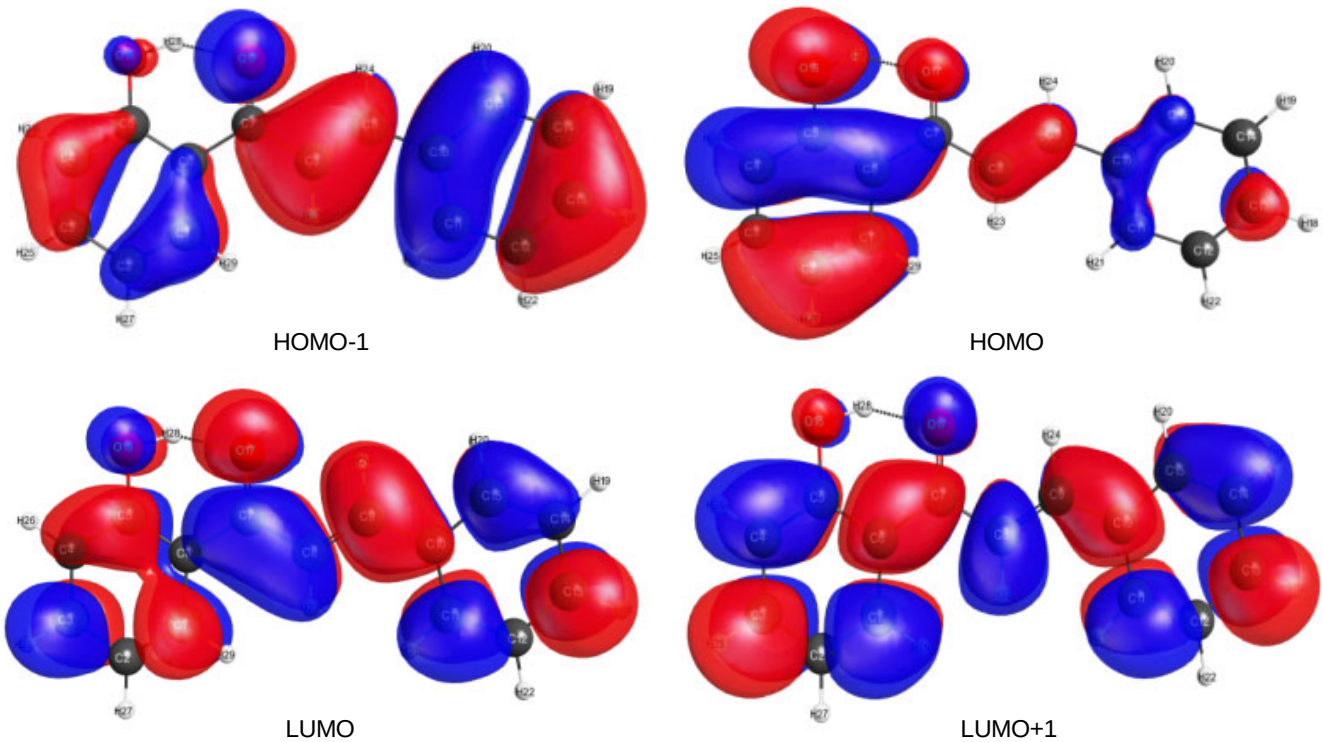

Fig. 3. Frontier molecular orbital's of 2'-HC molecule

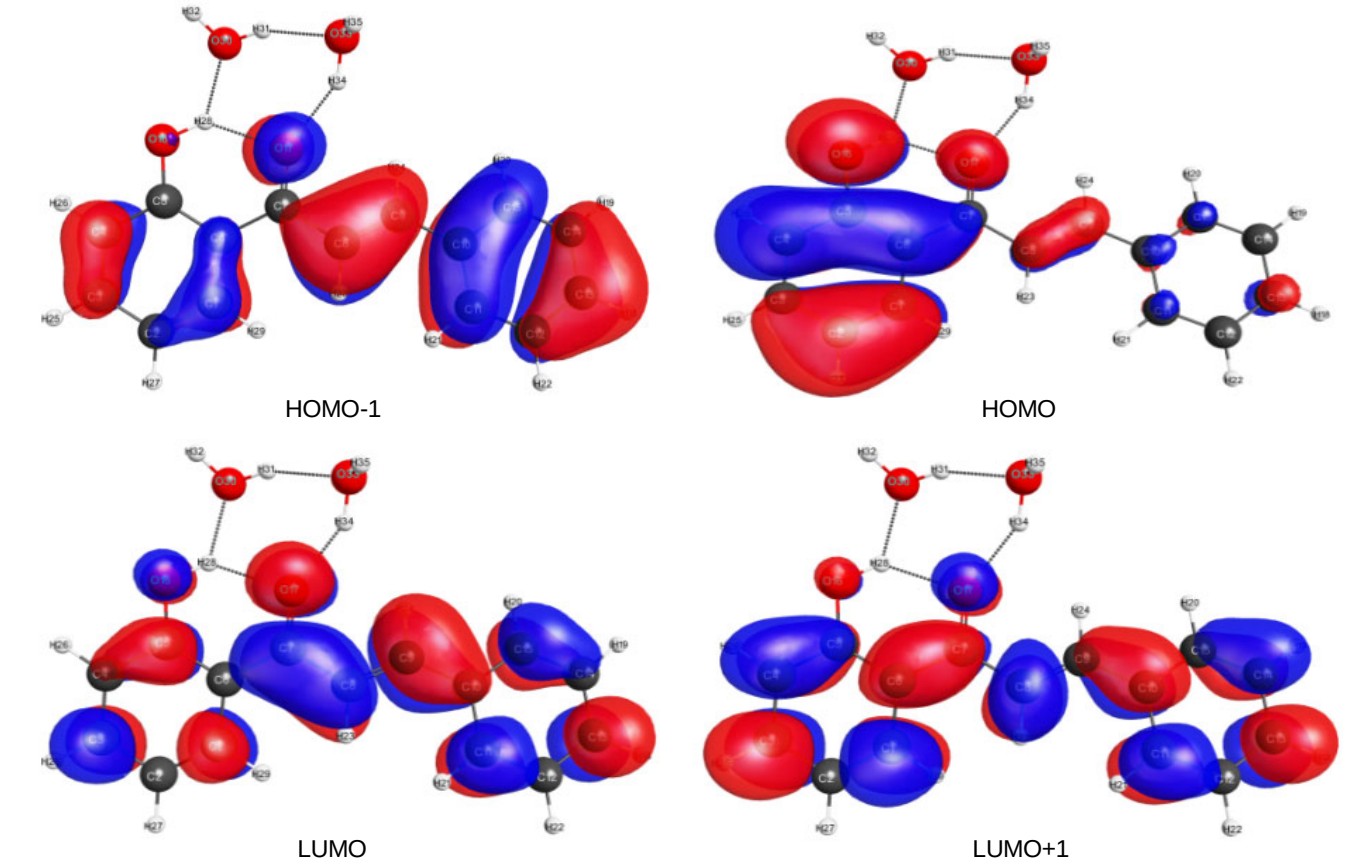

Fig. 4. Frontier molecular orbital's of 2'-HCH molecule

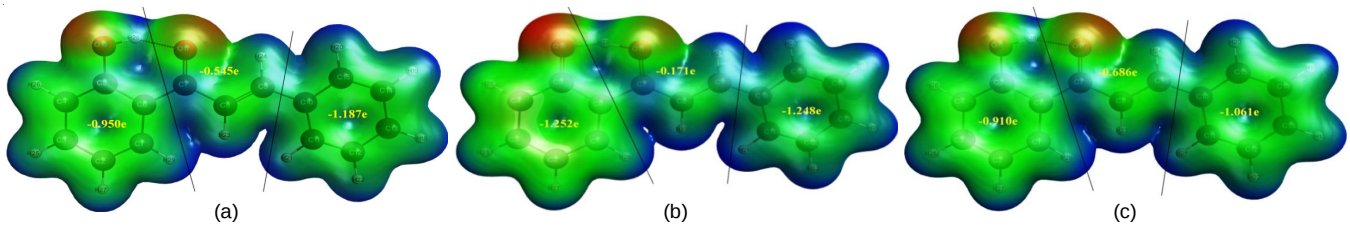

Fig. 5. MEP with charges on different atoms and groups for 2'-HC molecule at (a) S_0 (b) S_1 (c) S_3 states

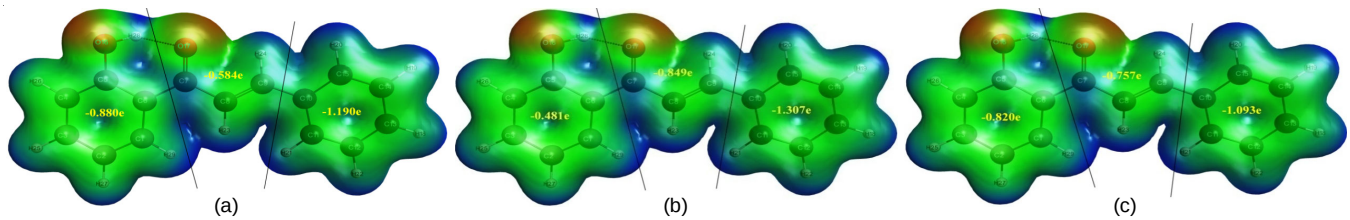

Fig. 6. MEP with charges on different atoms and groups for 2'-HCH molecule at (a) S_0 (b) S_1 (c) S_3 states

ethanol solvents are reckoned by using 6-31G(d,p)/TDDFT/EFP1/PCM method and the corresponding spectra have shown in Fig. 7. The UV-Vis-absorption spectra of 2′-HC and 2′-HCH molecules show two peaks corresponding to S_1 and S_3 states in the region between 280-420 nm. The absorption wavelengths corresponds to gas/water/ethanol solvents in S_1, S_3 states for 2′-HC are 287, 318/381.5, 333/382 and 333.1 nm and in 2′-HCH are 395.5, 314.3/379.7, 327.5/380.5 and 327.6 nm, respectively. A theoretical absorption wavelength of 382/333.1 nm in ethanol solvent is in good agreement with the experimentally determined value 366/316 nm [51] corresponds to S_1/S_3 states of 2′-HC molecule. The vertical absorption energies, oscillating strengths and probable wave functions are tabulated in Table-4.

Hydrogen bond dynamics: The HB-dynamics studies were done on pure and its water complex by employing DFT/TDDFT/PCM/EFP1 method at both ground and excited states. In pure and hydrated molecules, an intra-molecular HB O16-H28···O17=C7 exists between hydrogen (H28) of the hydroxyl group and oxygen (O17) of the carbonyl group of basic chalcone moiety. This intramolecular HB altered as O17-H28···O16

TABLE-4
PEAKS REPRESENTS THE THEORETICAL SIMULATED UV-VIS ABSORPTION SPECTRAL WAVELENGTHS (λ) 2′-HC AND 2′-HCH MOLECULES CORRESPONDS TO ELECTRONIC TRANSITIONS WITH OSCILLATOR STRENGTHS (f) IN GAS PHASE, WATER AND ETHANOL SOLVENTS

Molecule	Gas phase/solvents	Excited states	λ_a (nm)	f	Wave function (excitation amplitude)
2′-HC	Gas	S_1	387.0	0.172	H→L(-0.993), H-1→L(0.058)
		S_3	318.0	0.682	H→L(0.0729), H-1→L(0.959)
	Water	S_1	381.5	0.302	H→L(-0.993), H-1→L(-0.075)
		S_3	333.0	0.620	H→L(-0.082), H-1→L(0.948)
	Ethanol	S_1	382.0	0.305	H→L(0.993), H-1→L(-0.067)
		S_3	333.1	0.625	H→L(-0.074), H-1→L(-0.950)
2′-HCH	Gas	S_1	395.5	0.145	H→L(-0.994), H-1→L(-0.032)
		S_3	314.3	0.697	H→L(-0.046), H-1→L(0.938)
	Water	S_1	379.7	0.262	H→L(-0.995)
		S_3	327.5	0.620	H-1→L(-0.923)
	Ethanol	S_1	380.5	0.263	H→L(0.995)
		S_3	327.6	0.626	H-1→L(-0.924)

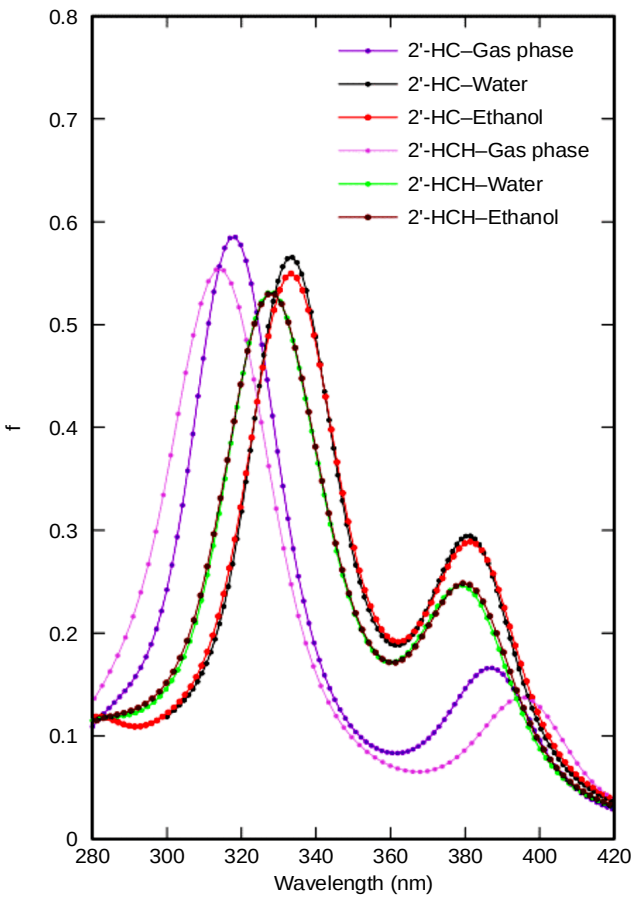

Fig. 7. UV-vis spectra of 2'-HC and 2'-HCH molecules in gas phase, water and ethanol solvents

=C5 in S_1 state due to hydrogen atom transfer, but not in the S_3 state of the pure molecule. In 2′-HCH molecule, two intermolecular HB's exist O16-H28···O30-H31 HB across hydrogen atom of hydroxyl group and C7=O17···H34-O33 HB across oxygen of carbonyl group. O30-H31···O33-H35 HB exists between water molecules both in ground and excited states. Due to the effect of microsolvation, intramolecular HB length increased by 0.237 Å. In S_1/S_3 states, intramolecular HB O16-H28···O17=C7 length decreased by 0.152/0.085 Å. The intermolecular HB O16-H28···O30-H31 length increased by 0.020 Å, 0.096 Å in S_1, the S_3 States and intermolecular HB C7=O17H34 -O33 length increased by 0.010 Å in S_1 state and decreased by 0.036 Å in S_3 state. The HB O30-H31···O33-H35 length decreased/increased by 0.031 Å/0.023 Å in S_1/S_3 states. The intramolecular and intermolecular HB lengths and dihedral angles across HB's of 2′-HC and 2′-HCH molecules at S_0, S_1 and S_3 states are tabulated in Tables 5 and 6.

ESIHT mechanism through PES scan: The intramolecular charge transfer state of 2′-HC is strongly sustained by the transfusing hydrogen atom (H28) from the hydroxyl group to the carbonyl group with the alteration of HB O16-H28··· O17=C7 to O17-H28···O16=C5. The ground and first excited state electronic PES scans of the H28 atom transferred path in the gas phase have been done with LR-TDDFT/6-31G (d,p)/ B3LYP method. The plots of potential energy alteration and the -OH bond (O16-H28) in 2′-HC molecule are presented in Fig. 8. The 2′-HC molecule can abide in an unrelaxed first excited state (S_1^*) by photo-excitation with absorbed energy 3.17 eV and the O16–H28 bond stretches to 1.620 Å, the H28 atom detached from O16 and bonded to O17. This point

TABLE-5
INTRA-MOLECULAR AND INTER-MOLECULAR HB LENGTHS OF 2′-HC AND 2′-HCH MOLECULES AT S_0, S_1 AND S_3 STATES

Hydrogen bond	2′-HC			2′-HCH		
	S_0	S_1	S_3	S_0	S_1	S_3
O16–H28···O17=C7	1.608	–	1.565	1.845	1.693	1.760
O17–H28···O16=C5	–	1.327	–	–	–	–
O16–H28···O30-H31	–	–	–	1.840	1.860	1.936
C7=O17···H34-O33	–	–	–	1.839	1.849	1.803
O30-H31···O33-H35(WB)	–	–	–	1.838	1.807	1.861

TABLE-6
DIHEDRAL ANGLES (°) ACROSS INTRA-MOLECULAR AND INTER-MOLECULAR HB LENGTH'S of 2′-HC AND 2′-HCH MOLECULES AT S_0, S_1 AND S_3 STATES

Hydrogen bond	2′-HC			2′-HCH		
	S_0	S_1	S_3	S_0	S_1	S_3
O16-H28···O17=C7	0	–	1.4	12.1	-4.6	9.9
O17-H28···O16=C5	–	6.2	–	–	–	–
O16-H28···O30-H31	–	–	–	151.0	158.5	152.5
C7=O17···H34-O33	–	–	–	159.9	145.5	151.6
O30-H31···O33-H35(WB)	–	–	–	106.3	104.7	102.5

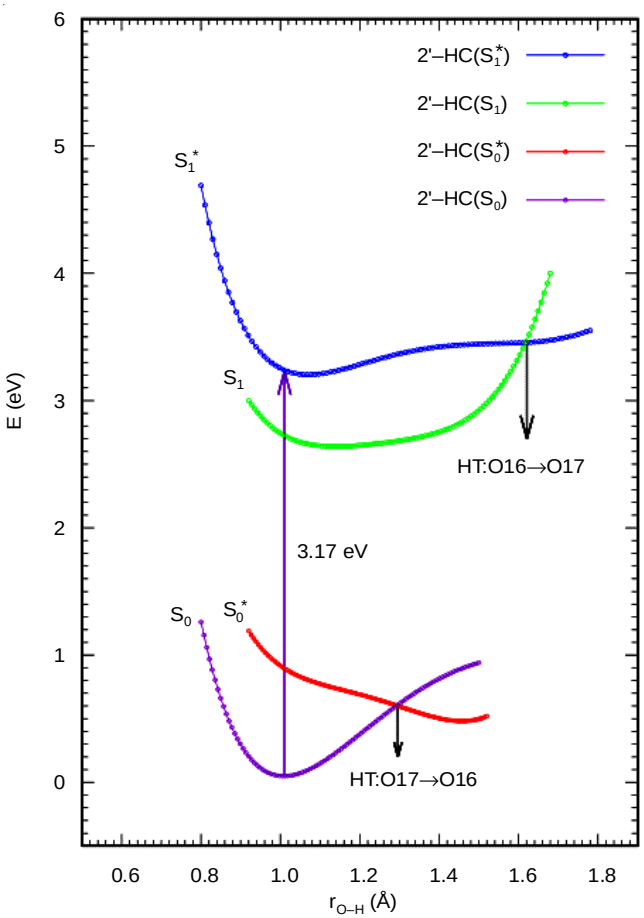

Fig. 8. Potential energy plot along intra-molecular hydrogen atom transfer path in 2'-HC molecule

corresponds to ESIHT. The 2′-HC molecule stabilizes in the relaxed first excited state (S_1) with O17–H28 bond length of 1.119 Å. The molecules are de-excited to the un-relaxed ground state (S_0 presented in Fig. 8). At this state, the O17–H28 bond length in 2′-HC molecule again stretches to 1.3 Å, where the expulsion of the H28 atom from O17 to O16 occurs and the molecule returns to its ground state (S_0).

Conclusion

In this theoretical work, ESIHT mechanisms have been investigated in the S_1 state of 2′-hydroxychalcone (2′-HC) by DFT/TDDFT/B3LYP/6-31G(d,p) method. PES scan establishes the intramolecular hydrogen atom transfer from hydroxyl to a carbonyl group on excitation of 2′-HC from $S_0 \rightarrow S_1$ state, but not in $S_0 \rightarrow S_3$ state. It is also inspected that in the micro-solvated molecule, no hydrogen atom transfer takes place from $S_0 \rightarrow S_1$/S_3 states. It is observed that the hydration of 2′-HC molecule using the EFP1 method insinuates the probability of two intermolecular hydrogen bonding sites. And also, there is a good agreement between the computed experimental absorption wavelength of 2′-HC in ethanol was obtained with a difference of (16 nm/17.1 nm) in (S_1/S_3) states. The molecular orbital's, MEP plots and natural charge analysis of both 2′-HC and 2′-HCH molecules elucidate the study of the molecules' intramolecular charge transfer (ICT) state. The ESIHT mechanism study affords the ongoing research on the biological and chemical activity of many hydroxy chalcones and their derivatives.

CONFLICT OF INTEREST

The authors declare that there is no conflict of interests regarding the publication of this article.

REFERENCES

1. Y. Liu, J. Ding, R. Liu, D. Shi and J. Sun, *J. Photochem. Photobiol. Chem.*, **201**, 203 (2009); https://doi.org/10.1016/j.jphotochem.2008.10.016
2. P. Zhou, P. Song, J. Liu, K. Han and G. He, *Phys. Chem. Chem. Phys.*, **11**, 9440 (2009); https://doi.org/10.1039/b910043a
3. E. Pines, D. Pines, Y.Z. Ma and G.R. Fleming, *ChemPhysChem*, **5**, 1315 (2004); https://doi.org/10.1002/cphc.200301004
4. E.T.J. Nibbering, H. Fidder and E. Pines, *Rev. Phys. Chem.*, **56**, 337 (2005); https://doi.org/10.1146/annurev.physchem.56.092503.141314
5. G.J. Zhao and K.L. Han, *Acc. Chem. Res.*, **45**, 404 (2012); https://doi.org/10.1021/ar200135h
6. G.J. Zhao and K.L. Han, *J. Phys. Chem. A*, **111**, 9218 (2007); https://doi.org/10.1021/jp0719659
7. G.J. Zhao, J.Y. Liu, L.C. Zhou and K.L. Han, *J. Phys. Chem. B*, **111**, 8940 (2007); https://doi.org/10.1021/jp0734530
8. A. Morimoito, T. Yatsuhashi, T. Shimada, L. Biczók, D.A. Tryk and H. Inoue, *J. Phys. Chem. A*, **105**, 10488 (2001); https://doi.org/10.1021/jp0117213
9. L. Biczok, T. Berces and H. Linschitz, *J. Am. Chem. Soc.*, **119**, 11071 (1997); https://doi.org/10.1021/ja972071c
10. V. Vetokhina, M. Kijak, G. Wiosna-Salyga, R.P. Thummel, J. Herbich and J. Waluk, *Photochem. Photobiol. Sci.*, **9**, 923 (2010); https://doi.org/10.1039/c0pp00043d
11. G.J. Zhao and K.L. Han, *ChemPhysChem*, **9**, 1842 (2008); https://doi.org/10.1002/cphc.200800371
12. K.L. Han and G.J. Zhao, Hydrogen Bonding Transfer in the Excited State. John Wiley & Sons Ltd. (2011).
13. G.Y. Li, Y.H. Li, H. Zhang and G.H. Cui, *Commun. Comput. Chem.*, **1**, 88 (2013); https://doi.org/10.4208/cicc.2013.v1.n1.9

14. G.J. Zhao and K.L. Han, *Biophys. J.*, **94**, 38 (2008); https://doi.org/10.1529/biophysj.107.113738
15. S. Banerjee, A.K. Both and M. Sarkar, *ACS Omega*, **3**, 15709 (2018); https://doi.org/10.1021/acsomega.8b02232
16. H. Wang, M. Wang, E. Liu, M. Xin and C. Yang, *Comput. Chem.*, **964**, 243 (2011); https://doi.org/10.1016/j.comptc.2010.12.034
17. H. Wang, M. Wang, M. Xin, E. Liu and C. Yang, *Cent. Eur. J. Phys.*, **9**, 792 (2011); https://doi.org/10.2478/s11534-010-0099-4
18. G. Jones II, W.R. Jackson and A.M. Halpern, *Chem. Phys. Lett.*, **72**, 391 (1980); https://doi.org/10.1016/0009-2614(80)80314-9
19. M.J. Kamlet, C. Dickinson and R.W. Taft, *Chem. Phys. Lett.*, **77**, 69 (1981); https://doi.org/10.1016/0009-2614(81)85602-3
20. P. Arora, L.V. Slipchenko, S.P. Webb, A. DeFusco and M.S. Gordon, *J. Phys. Chem. A*, **114**, 6742 (2010); https://doi.org/10.1021/jp101780r
21. N. De Silva and F. Zahariev, *J. Chem. Phys.*, **134**, 54111 (2011); https://doi.org/10.1063/1.3523578
22. S. Yoo, F. Zahariev, S. Sok and M.S. Gordon, *J. Chem. Phys.*, **129**, 144112 (2008); https://doi.org/10.1063/1.2992049
23. P.N. Day, J.H. Jensen, M.S. Gordon, S.P. Webb, W.J. Stevens, M. Krauss, D. Garmer, H. Basch and D. Cohen, *J. Chem. Phys.*, **105**, 1968 (1996); https://doi.org/10.1063/1.472045
24. M.S. Gordon, M.A. Freitag, P. Bandyopadhyay, J.H. Jensen, V. Kairys and W.J. Stevens, *J. Phys. Chem. A*, **105**, 293 (2001); https://doi.org/10.1021/jp002747h
25. M.A. Adamovic, M.A. Freitag and M.S. Gordon, *J. Chem. Phys.*, **118**, 6725 (2003); https://doi.org/10.1063/1.1559912
26. J.H. Jensen and M.S. Gordon, *J. Chem. Phys.*, **108**, 4772 (1998); https://doi.org/10.1063/1.475888
27. K. Goyal, R. Kaur, A. Goyal and R. Awasthi, *J. Appl. Pharm. Sci*., **11**, 1 (2021); https://doi.org/10.7324/JAPS.2021.11s101
28. H. Koudokpon, N. Armstrong, T.V. Dougnon, L. Fah and J.M. Rolain, *BioMed Res. Int.*, **2018**, 1453173 (2018); https://doi.org/10.1155/2018/1453173
29. D. Elkhalifa, I. Al-Hashimi, A.-E. Al-Moustafa and A. Khalil, *J. Drug Target.*, **29**, 403 (2021); https://doi.org/10.1080/1061186X.2020.1853759
30. M. Xu, P. Wu, F. Shan, J. Ji and K.P. Rakesh, *Bioorg. Chem.*, **91**, 103133 (2019); https://doi.org/10.1016/j.bioorg.2019.103133
31. S.-M. Yun, S.-H. Kim and E.-H. Kim, *Front. Pharmacol.*, **10**, 162 (2019); https://doi.org/10.3389/fphar.2019.00162
32. Y. Xue, Y. Zheng, L. Zhang, W. Wu, D. Yu and Y. Liu, *J. Mol. Model.*, **19**, 3851 (2013); https://doi.org/10.1007/s00894-013-1921-x
33. F.-W. Wang, S.-Q. Wang, B.-X. Zhao and J.-Y. Miao, *Org. Biomol. Chem.*, **12**, 3062 (2014); https://doi.org/10.1039/C3OB42429D
34. M. Dommetta and R. Crespo-Otero, *Phys. Chem. Chem. Phys.*, **19**, 2409 (2016); https://doi.org/10.1039/C6CP07541J
35. C. Simmler, A. Hajirahimkhan, D.C. Lankin, J.L. Bolton, T. Jones, D.D. Soejarto, S.-N. Chen and G.F. Pauli, *J. Agric. Food Chem.*, **61**, 2146 (2013); https://doi.org/10.1021/jf304445p
36. M.D. Hanwell, D.E. Curtis, D.C. Lonie, T. Vandermeersch, E. Zurek and G.R. Hutchison, *J. Cheminform.*, **4**, 17 (2012); https://doi.org/10.1186/1758-2946-4-17
37. W. Kohn, A.D. Becke and R.G. Parr, *J. Phys. Chem.*, **100**, 12974 (1996); https://doi.org/10.1021/jp9606691
38. K. Kim and K.D. Jordan, *J. Phys. Chem.*, **98**, 10089 (1994); https://doi.org/10.1021/j100091a024
39. P.J. Stephens, F.J. Devlin, C.F. Chabalowski and M.J. Frisch, *J. Phys. Chem.*, **98**, 11623 (1994); https://doi.org/10.1021/j100096a001
40. A.D. Becke, *J. Chem. Phys.*, **109**, 2092 (1998); https://doi.org/10.1063/1.476722
41. S. Tokura, T. Sato, T. Tsuneda, T. Nakajima and K.J. Hirao, *Comput. Chem.*, **29**, 1187 (2008); https://doi.org/10.1002/jcc.20871
42. M. Chiba, T. Tsuneda and K. Hirao, *J. Chem. Phys.*, **124**, 144106 (2006); https://doi.org/10.1063/1.2186995
43. A.D. Becke, *Phys. Rev. A*, **38**, 3098 (1988); https://doi.org/10.1103/PhysRevA.38.3098
44. F. Furche and R. Ahlrichs, *J. Chem. Phys.*, **121**, 12772 (2004); https://doi.org/10.1063/1.1824903
45. D. Si and H. Li, *J. Chem. Phys.*, **133**, 144112 (2010); https://doi.org/10.1063/1.3491814
46. J. Perdew, M. Ernzerhof and K. Burke, *J. Chem. Phys.*, **105**, 9982 (1996); https://doi.org/10.1063/1.472933
47. E.D. Glendening, C.R. Landis and F. Weinhold, *Comput. Mol. Sci.*, **2**, 1 (2012); https://doi.org/10.1002/wcms.51
48. M.W. Schmidt, K.K. Baldridge, J.A. Boatz, S.T. Elbert, M.S. Gordon, J.H. Jensen, S. Koseki, N. Matsunaga, K.A. Nguyen, S. Su, T.L. Windus, M. Dupuis and J.A. Montgomery, *J. Comput. Chem.*, **14**, 1347 (1993); https://doi.org/10.1002/jcc.540141112
49. M.S. Gordon and M.W. Schmidt, Eds.: In: C.E. Dykstra, G. Frenking, K.S. Kim and G.E. Scuseria,Advances in Electronic Structure Theory: GAMESS A Decade Later; In: Theory and Applications of Computational Chemistry: The First Forty Years, Elsevier, Amsterdam, Ed. 1, pp. 1167-1189 (2005).
50. P.C. Hariharan and J.A. Pople, *Theor. Chim. Acta*, **28**, 213 (1973); https://doi.org/10.1007/BF00533485
51. F. Leonard, A. Wajngurt, M. Klein and C.M. Smith, *J. Org. Chem.*, **26**, 4062 (1961); https://doi.org/10.1021/jo01068a101